Development 140, 4008-4019 (2013) doi:10.1242/dev.095034

Chromatin reprogramming during the somatic-to-reproductive cell fate transition in plants

Wenjing She[1], Daniel Grimanelli[2], Kinga Rutowicz[3], Marek W. J. Whitehead[1], Marcin Puzio[3], Maciej Kotliński[3], Andrzej Jerzmanowski[3] and Célia Baroux[1,*]

SUMMARY

The life cycle of flowering plants is marked by several post-embryonic developmental transitions during which novel cell fates are established. Notably, the reproductive lineages are first formed during flower development. The differentiation of spore mother cells, which are destined for meiosis, marks the somatic-to-reproductive fate transition. Meiosis entails the formation of the haploid multicellular gametophytes, from which the gametes are derived, and during which epigenetic reprogramming takes place. Here we show that in the *Arabidopsis* female megaspore mother cell (MMC), cell fate transition is accompanied by large-scale chromatin reprogramming that is likely to establish an epigenetic and transcriptional status distinct from that of the surrounding somatic niche. Reprogramming is characterized by chromatin decondensation, reduction in heterochromatin, depletion of linker histones, changes in core histone variants and in histone modification landscapes. From the analysis of mutants in which the gametophyte fate is either expressed ectopically or compromised, we infer that chromatin reprogramming in the MMC is likely to contribute to establishing postmeiotic competence to the development of the pluripotent gametophyte. Thus, as in primordial germ cells of animals, the somatic-to-reproductive cell fate transition in plants entails large-scale epigenetic reprogramming.

KEY WORDS: *Arabidopsis*, Plant reproduction, Megaspore mother cell, Heterochromatin, Chromatin modifications, Histone variants

INTRODUCTION

In sexually reproducing organisms, gametes are generated by a specific lineage derived from somatic cells that undergo a somatic-to-reproductive cell fate transition (SRT). In mammals, the primordial germ cells (PGCs) differentiate in the embryo at gastrulation stage (Bendel-Stenzel et al., 1998). By contrast, the spore mother cells (SMCs) of flowering plants are formed in the adult plant during floral organ differentiation (Maheshwari, 1950). The female SMC, or megaspore mother cell (MMC), differentiates from nucellar cells within the ovule primordium. The male SMC, or microspore mother cell, develops from the sporogeneous tissue within the anthers. Unlike in animals, the plant products of meiosis (spores) do not directly give rise to functional gametes. Instead, they undergo mitosis to form multicellular structures called gametophytes, which, in turn, give rise to the gametes. In most flowering plants, such as in *Arabidopsis*, the gametophytes are reduced to a small number of cells. The male gametophyte, or pollen, is composed of two sperm cells enclosed within a vegetative cell. The female gametophyte, or embryo sac, is composed of two gametes, termed the egg and central cell, accompanied by accessory cells called antipodals and synergids, the latter of which assist in fertilization. Double fertilization encompasses two fertilization events that produce a totipotent zygote and a nourishing tissue termed the endosperm.

[1]Institute of Plant Biology and Zürich-Basel Plant Science Center, University of Zürich, Zollikerstrasse 107, 8008 Zürich, Switzerland. [2]Institut de Recherche pour le Développement (UMR 232), Centre National de la Recherche Scientifique (URL 5300), Université de Montpellier II, 911 Avenue Agropolis, 34394 Montpellier, France. [3]Laboratory of Plant Molecular Biology, Warsaw University and Institute of Biochemistry and Biophysics, Polish Academy of Sciences, Pawińskiego 5a, 02-106 Warsaw, Poland.

*Author for correspondence (cbaroux@botinst.uzh.ch)

Accepted 15 July 2013

Plant gametophyte development establishes several cell types with distinct fates over the course of only two to three divisions. For the female gametophyte, which initiates its polarized development as a syncythium, it has been postulated that epigenetic differentiation of the mitotic daughter nuclei might already take place in nuclei before cellularization (Messing and Grossniklaus, 1999; Grant-Downton and Dickinson, 2006). There is a growing body of evidence that gametophyte development is associated with nuclear-scale epigenome remodeling. Dynamic patterns of DNA methyltransferase expression, DNA methylation, and in the distribution of histone variants and histone modifications have been described at discrete stages of embryo sac and pollen development (Ingouff et al., 2007; Schoft et al., 2009; Ingouff et al., 2010; Pillot et al., 2010; Houben et al., 2011; Ibarra et al., 2012; Jullien et al., 2012). Ultimately, an epigenetic dimorphism is established at the level of DNA methylation, histone modifications and their readers, histone variants and transcriptional competence in mature gametophytes, both between the sperm and vegetative cell in the pollen and between the egg and central cell in the embryo sac. This dimorphism is thought to play important functional roles, including the control of transcriptional activity in the egg and early embryo (Pillot et al., 2010) and of transposable elements in the gametes and early embryo, guided by small RNAs (Slotkin et al., 2009; Calarco and Martienssen, 2011; Ibarra et al., 2012). Another wave of reprogramming occurs after fertilization, with the renewal of the repertoire of histone H3 variants in the zygote and the resetting of DNA methylation patterns during the first divisions of the embryo (Ingouff et al., 2010; Jullien et al., 2012).

Thus, two windows of reprogramming have been described during plant reproduction to date: first, during postmeiotic gametophyte development and second, after fertilization during seed development. However, whether reprogramming occurs before meiosis in the SMCs is unknown. In animals, epigenetic reprogramming at the equivalent stage of reproduction, in the PGCs, is crucial for subsequent development. In plants, genetic evidence

indicates that small-RNA-dependent DNA methylation pathways acting in the nucellus surrounding the MMC play a key role both during MMC specification (Olmedo-Monfil et al., 2010; Singh et al., 2011) and later for the initiation of female gametophyte development (Tucker et al., 2012). In addition, SMC differentiation is characterized by elevated transcriptional levels for many of the enzymes that participate in epigenetic regulatory pathways (Berger and Twell, 2011; Schmidt et al., 2011), although their effects on SMC chromatin, as well as their functions in spore and gamete development, remain poorly understood.

Thus, an unresolved question is whether the specification of SMCs, which marks the SRT, coincides with a window of epigenetic reprogramming or whether reprogramming is a sole attribute of postmeiotic development. Here, we analyzed nuclear organization and chromatin composition in the differentiating MMC of *Arabidopsis*. We found highly dynamic chromatin changes coinciding with a slow meiotic S phase, suggesting reprogramming of the epigenetic landscape during MMC specification. Based on the analysis of various mutants, we inferred that these events contribute to the acquisition of the gametophyte fate.

MATERIALS AND METHODS

Plant material and growth conditions

Arabidopsis plants were grown under long-day conditions (16 hours light) at 18-20°C in a plant growth chamber or greenhouse, except for the mutants *ago9-4*, *sgs3-11* and *rdr6-2* (Olmedo-Monfil et al., 2010), which were grown at 23°C in a growth incubator (Percival). The GFP lines shown Fig. 2 and supplementary material Fig. S1 are the following: HTR5-GFP is pHTR5::HTR5-GFP and HTR8-GFP is pHTR8::HTR8-CFP (Ingouff et al., 2010); H2A.Z-GFP is pHTA11::HTA11-GFP (Kumar and Wigge, 2010); HTR12-GFP and GFP-HTR12 (CENH3 lines) are pHTR12::HTR12-GFP (Fang and Spector, 2005) and pCENH3::GFP-CENH3 (Ravi et al., 2011), respectively; LHP1-GFP line is pLHP1::LHP1-GFP (Nakahigashi et al., 2005). A full description of N- and C-terminal fusions of H1 variants with GFP, CFP or RFP is available upon request. In brief, the coding sequence, promoter and 3′UTR (termination) sequences of H1.1 and H1.2 were amplified separately using the primers described in supplementary material Table S8 and subcloned into either pCAMBIA1390 (C-terminal fusions) or a modified pCAMBIA1390 vector where the 35S::HygR resistance cassette has been replaced by a NOS::BAR resistance cassette from pGREENII 029 (Hellens et al., 2000). The EGFP and CFP sequences were subcloned and the RFP-T sequence amplified from the pRFP-T_tag plasmid (Shaner et al., 2008). We analyzed four and six independent lines carrying N- and C-terminal GFP fusions of the H1.1 variant in the *h1.1* mutant background, respectively, three each of N- and C-terminal EGFP fusions to the H1.2 variant, as well as six N-terminal CFP fusions to H1.2 and ten C-terminal RFP fusions to H1.1. For Syringolin A treatment, whole inflorescences were cut and incubated in water (mock) or 100 nM Syringolin A (Groll et al., 2008) in water and placed in the growth chamber for 48 hours before imaging.

Immunostaining in whole-mount ovule primordia

Immunostaining of active PolII was performed as previously described using the anti-RNA Pol II [phospho-S2] antibody (Abcam, ab24758) (Autran et al., 2011). A detailed protocol for immunostaining of histone modifications, H3 and H1 will be published elsewhere. In brief, young carpels were fixed with 1% formaldehyde and 10% DMSO in PBS-Tween (0.1%) before dissection and embedding of the ovule primordia in 5% acrylamide pads on microscope slides. Tissue processing included clarification (methanol/xylene), cell wall digestion and permeabilization before application of the primary, then secondary antibody for 12-14 hours at 4°C. The samples were counterstained with propidium iodide and mounted in Prolong Gold (Invitrogen). Immunostaining efficiency was tested using serial dilutions of the primary antibodies (1:200, 1:500, 1:1000) and the lowest dilution that gave reproducible and homogenous signals was chosen for quantitative imaging (supplementary material Table S7). Control immunodetection in the absence of primary antibody was also performed. The antibodies used are described in supplementary material Table S7.

EdU labeling

A 5-ethynyl-2′-deoxyuridine (EdU)-based assay for S-phase detection was performed as described (Kotogany et al., 2010). Whole inflorescences were incubated in 100 μM EdU solution (Invitrogen, A10044) for 2 hours at 23°C in a plant growth incubator (Percival), then fixed in 4% formaldehyde and 0.1% Triton X-100 in PBS (15 minutes at room temperature), and washed three times in PBS (5 minutes each). Fluorescent labeling of EdU was performed for 30 minutes at room temperature in the dark, followed by three washes in PBS supplemented with 100 ng/ml DAPI. Ovule primordia were then dissected from the carpels and mounted on slides with DAPI in Vectashield (Vector Labs).

Image acquisition and quantitative analyses

Serial images of fluorescent signals in whole-mount ovule primordia were recorded by confocal laser-scanning microscopy with a Leica IRE-SP2 and SP5-R (Leica Microsystems) using a 63× GLY lens (glycerol immersion, NA 1.4). Antibody and DNA signals were acquired sequentially and the volumes were sampled according to the Nyquist rate (2× oversampling). Zoom factor, image geometry, voxel size, scanning speed and averaging were kept identical for the image series in an experiment. Fluorescent signals (GFP, antibody staining, DNA staining) were reported as the intensity sum of voxels per channel in nuclei in 3D-reconstructed images, using manually defined 3D surfaces around MMCs and nucellar nuclei [manual segmentation of nuclear surface using the Surface tool from Imaris software (Bitplane)]. Relative levels of histone H3 and H3 modifications were calculated as a ratio of the intensity sum in the antibody channel over that in the DNA staining channel. For nuclear measurements (as in Fig. 1), the nuclear volume was derived from the statistics of the contours drawn in Imaris, the chromatin volume was derived by subtracting the nucleolus volume (devoid of DNA signal) from that of the nucleus, and heterochromatin content and chromocenter number were calculated as described (Baroux et al., 2007): measurements were made using ImageJ on intensity sum projections from 3D series encompassing (non-overlapping) MMC and nucellus nuclei. The relative heterochromatin fraction (RHF) consisted of the sum of intensity signals in chromocenters (contours defined manually) expressed as a percentage of the total nuclear fluorescence intensity. Quantitative differences were assessed using a Welch's *t*-test (two-tailed).

RESULTS

MMC differentiation is marked by chromatin decondensation and reduction in heterochromatin

The differentiation of the MMC in the ovule primordium marks the onset of female reproductive lineage development. The MMC originates from a single cell in a subepidermal position in the nucellus and is located along the vertical, central axis of the ovule primordium (Fig. 1A) (Schneitz et al., 1995; Yang and Sundaresan, 2000). It undergoes progressive cellular differentiation during primordium growth over a period of 2-3 days before the onset of chromosome condensation during meiotic prophase (Fig. 1A,B). Previous histological studies showed that MMC differentiation is marked by cell enlargement and elongation (Schneitz, 1995) (Fig. 1A) as well as by changes in nuclear and nucleolar size (Cooper, 1937; Schulz and Jensen, 1981; Armstrong and Jones, 2003; Sniezko, 2006) (Fig. 1B-D; supplementary material Table S1). Using non-denaturing whole-mount DNA staining and confocal imaging, we measured a doubling in nuclear volume (Fig. 1C), which appeared to result from both nucleolus enlargement (Fig. 1A) and chromatin decondensation (Fig. 1D). This event coincides with a 60% reduction in heterochromatin content (Fig. 1E) and a decreased number of chromocenters (Fig. 1F). The nuclear organization of the MMC thus markedly differs from that of the surrounding nucellar cells, and nuclear differentiation is visible as

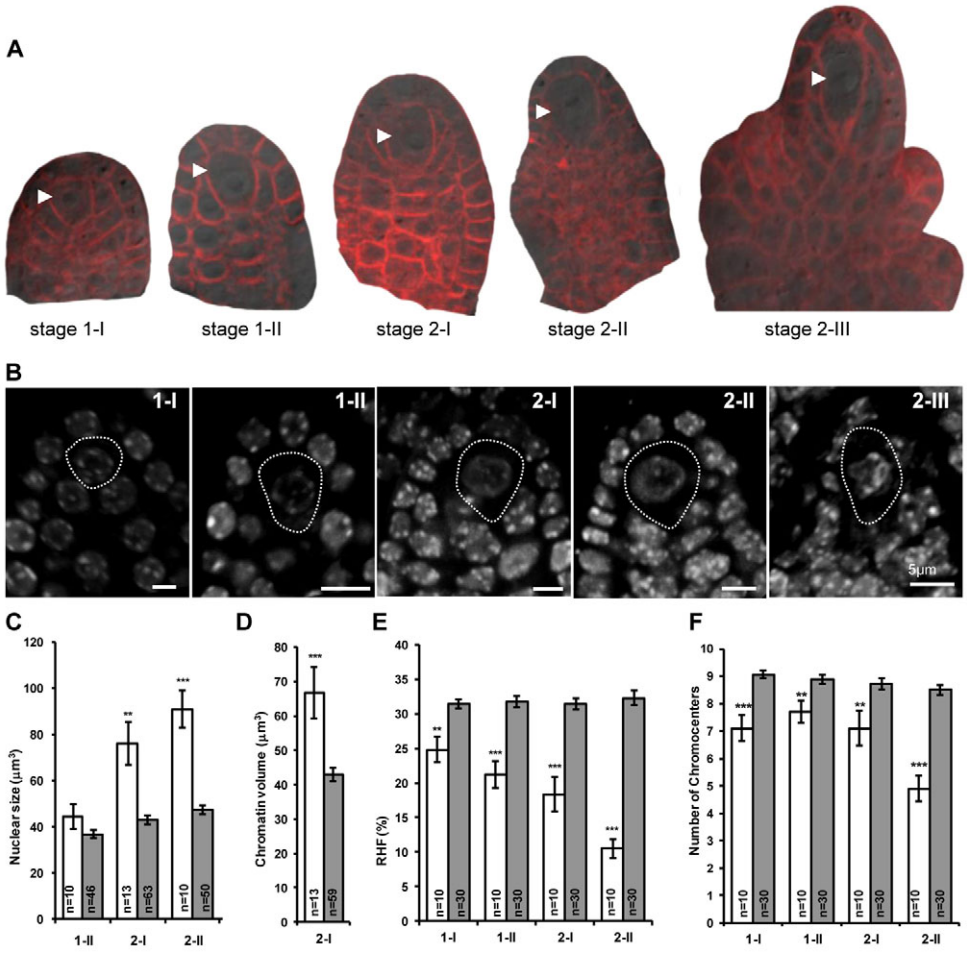

Fig. 1. Nuclear reorganization during MMC specification. (**A**) MMC differentiation in developing *Arabidopsis* ovule primordia at stages 1-I to 2-III (onset of meiosis) as defined by Schneitz et al. (Schneitz et al., 1995). The MMC (arrow) differentiates in a central, subepidermal position in the nucellus. Images are overlays of differential interference contrast (DIC) and FM4-64 counterstaining (red) photographs. (**B**) Whole-mount DNA staining (propidium iodide) allows 3D measurements of nuclear size and heterochromatin organization (C-F) in the MMC (outlined) compared with the surrounding nucellus cells. Partial projections of serial confocal sections are shown. (**C-F**) Quantitative analyses on 3D reconstructions provide measures of nuclear volume (C), chromatin volume (volume of nucleus minus nucleolus) (D), heterochromatin content (E; RHF, relative heterochromatin fraction) and chromocenter number (F). MMC, white bars; nucellus, gray bars. Stages are indicated on the *x*-axis and the number of nuclei analyzed is indicated in each bar (*n*). Error bars indicate s.e.m. Differences between the nucellus and MMC chromatin were assessed using a two-tailed Welch's *t*-test (**P*<0.05, ***P*<0.01, ****P*<0.001). Detailed quantifications are provided in supplementary material Table S1. Scale bars: 5 µm.

early as stage 1-I, when cell enlargement is also first observed, suggesting an early establishment of an MMC-specific chromatin state.

Histone variants are dynamically exchanged in differentiating MMCs

Linker histones (H1) are essential modulators of chromatin compaction through binding to the linker DNA and the core nucleosome, thereby stabilizing higher-order chromatin structure (Robinson and Rhodes, 2006). The *Arabidopsis* genome encodes three canonical variants (H1.1, H1.2, H1.3), which are broadly expressed during plant development, except for the stress-inducible H1.3 (Ascenzi and Gantt, 1997; Wierzbicki and Jerzmanowski, 2005). To determine whether chromatin decondensation in the MMC correlates with changes in H1 levels, we analyzed the dynamic localization of GFP-tagged variants in developing ovule primordia. We found a sharp decrease of H1.1-GFP and H1.2-GFP levels in MMCs at stage 1-I and undetectable levels at the consecutive stage (Fig. 2A,B). H1.3-GFP was never detected in primordia during MMC differentiation (not shown). The loss of H1.1 and H1.2 is, however, transient: *de novo* incorporation was observed at stages 2-II and 2-III, respectively, and throughout meiosis (supplementary material Fig. S1), consistent with a role of H1 in chromosome condensation. Immunostaining using a novel antibody raised against tobacco H1 confirmed the H1 depletion in the MMC observed with the GFP-tagged lines (supplementary material Fig. S2). Interestingly, the loss of H1 was strongly retarded in the presence of Syringolin A, a potent inhibitor of the plant proteasome (Groll et al., 2008) (Fig. 2C; supplementary material Fig. S3), suggesting the existence of active protein degradation mechanisms controlling H1 depletion from the MMC chromatin. In addition to linker histones, we also analyzed the nuclear distribution of a GFP-tagged variant of LIKE HETEROCHROMATIN PROTEIN1 [LHP1; also known as TERMINAL FLOWER2 (TFL2)], which, in contrast to HP1 in animals, localizes preferentially in euchromatic domains and influences chromatin accessibility (Maison and Almouzni, 2004; Libault et al., 2005; Nakahigashi et al., 2005; Turck et al., 2007). LHP1-GFP signals decreased significantly, although variably, by ~30-60% at stage 2-II (Fig. 2D).

Similarly, we analyzed H3 variants, encoded by the *HISTONE THREE RELATED* (*HTR*) gene family in *Arabidopsis*, fused in frame with fluorescent proteins. HTR12 is the *Arabidopsis* homolog of the centromere-specific variant CENH3 (Talbert et al., 2002). When we examined a C-terminal HTR12-GFP fusion (Fang and Spector, 2005), we observed a drastic depletion from the MMC chromatin at stage 1-II (Fig. 2E). HTR12-GFP signals were faintly recovered just before and at prophase I, although they showed a diffuse distribution at the latter stage (supplementary material Fig. S1). By contrast, the N-terminal GFP-HTR12 fusion (Ravi et al., 2011) showed persistent signals throughout MMC development and, as expected, conspicuous signals in prophase I (Fig. 2F; supplementary material Fig. S1). CENH3/HTR12 reloading has been shown to share structural requirements during male meiosis (as opposed to during mitosis) (Ravi et al., 2011). We thus hypothesized that the MMC chromatin might undergo a rapid turnover of CENH3, whereby the C-terminal

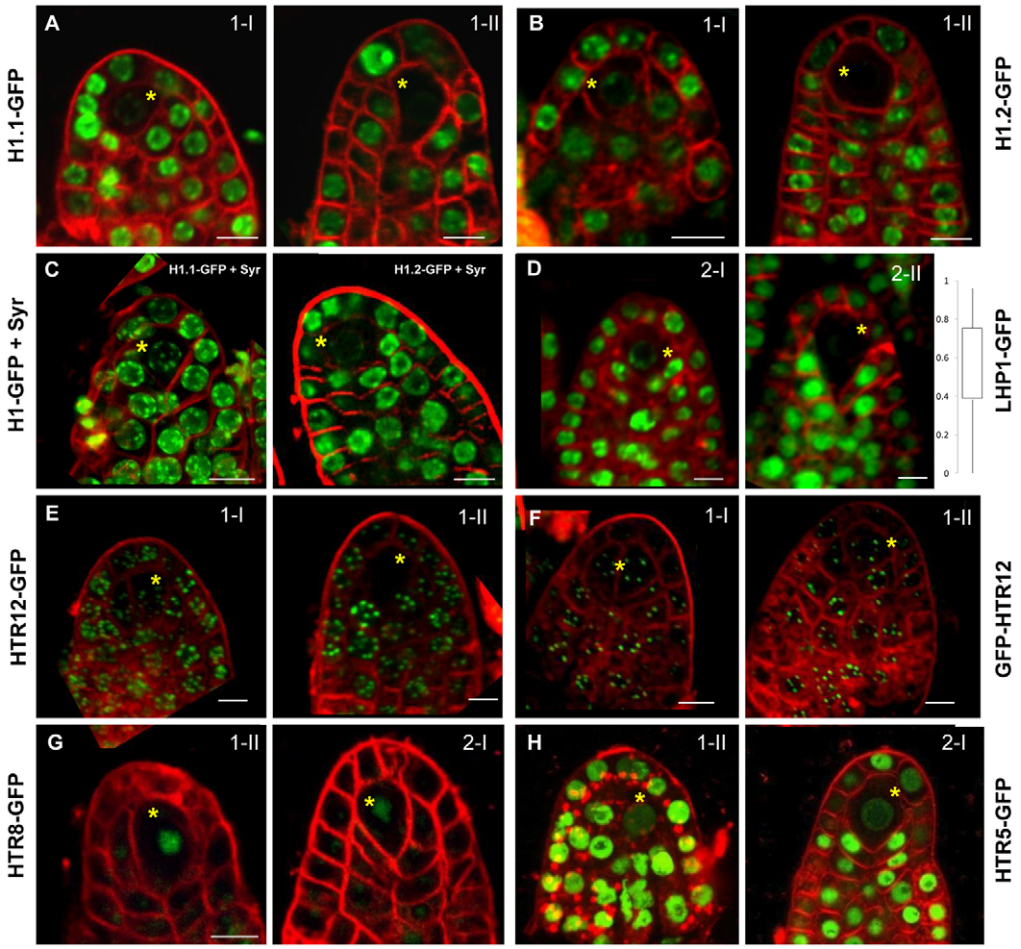

Fig. 2. Dynamics of H1 and H3 histone variants and LHP1 during MMC differentiation. The dynamic nuclear distribution during MMC differentiation of various GFP-tagged chromatin components. (**A-C**) Linker histone variants H1.1 and H1.2 in wild-type MMCs (A,B) and in MMCs exposed to 100 nM Syringolin A, a potent inhibitor of the plant proteasome, for 48 hours (C). (**D**) Chromatin-associated protein LHP1. (**E**,**F**) Centromeric H3 variant CENH3/HTR12 as N-terminal (E) or C-terminal (F) fusions. (**G**,**H**) H3.3 variants HTR8 (G) and HTR5 (H). Green, GFP fluorescence; red, FM4-64 fluorescence. Asterisks indicate the MMC. For LHP1 (D), reduced levels in stages 2-I and 2-II were revealed upon signal quantification on 3D reconstructions. The box plot shows the fluorescence intensity ratios between MMC (n=12) and nucellus (n=44) chromatin (whiskers are upper and lower quartiles). The dynamic distribution of these GFP-tagged chromatin proteins throughout the entire phase of MMC development, meiosis and the FMS is shown in supplementary material Fig. S1. Scale bars: 5 μm.

fusion was improperly reloaded in the MMC following eviction, as has been described in male meiocytes (Ravi et al., 2011). By contrast, we also observed HTR8 and HTR5 (Ingouff et al., 2010) in the MMC (Fig. 2G,H), two H3.3 variants that are usually associated with transcriptional competence (Ahmad and Henikoff, 2002; Mito et al., 2005; Wollmann et al., 2012). This also indicates that loss of GFP signals in the MMC observed for the other histone-tagged variants is not an artifact.

Finally, changes in the repertoire of histone variants also encompassed H2A.Z, a labile variant that marks poised genes involved in rapid environmental responses (Deal and Henikoff, 2010; Kumar and Wigge, 2010; Coleman-Derr and Zilberman, 2012). We observed that a GFP-tagged HTA11/H2A.Z variant was evicted from the MMC chromatin as early as stage 2-I, and then reincorporated prior to prophase I (supplementary material Fig. S1).

Collectively, the depletion of linker histones H1.1, H1.2, LHP1 and H2A.Z is consistent with a global pattern of chromatin decondensation in the MMC. The dynamics of HTR12/CENH3, of the HTR5 and HTR8 H3.3 variants and of HTA11/H2A.Z indicate that core nucleosomes are remodeled, illustrating a global yet specific chromatin reprogramming during MMC differentiation.

MMC chromatin differs from that of surrounding somatic cells by distinct levels of histone H3 and H4 modifications and active RNA polymerase II

The changes we observed in nuclear organization and chromatin condensation in MMCs suggest the establishment of an open, permissive chromatin state. This state is usually associated with, and mediated by, biochemical modifications of specific amino acid residues of nucleosomal histones. We thus analyzed the relative levels of histone modifications associated with either a permissive (H3K4me2, H3K4me3) or repressive (H3K27me3) environment of euchromatic regions in plant nuclei (Fuchs et al., 2006). We performed immunostaining on whole-mount ovule primordia and compared MMC chromatin with that of neighboring nucellar cells (Fig. 3; supplementary material Table S2). In particular, we determined the chromatin state of MMCs at the end of their differentiation, at stage 2-II and just prior to prophase I. Whereas H3 levels, which were used as a control, were similar in both cell types (Fig. 3A), there was a 2.7-fold enrichment of H3K4me3 levels and a 50% reduction of H3K27me3 levels in the MMC relative to cells of the nucellus (Fig. 3B,C). H3K27me3 levels were not affected in mutants lacking RELATIVE OF EARLY FLOWERING6 (REF6) activity, an enzyme that catalyses H3K27me2/me3 demethylation (Lu et al., 2011) (supplementary material Fig. S4), indicating that loss of H3K27me3 in the MMC is either passive or mediated by another, as yet unknown, histone demethylase. Similarly, in mutants lacking TRITHORAX-RELATED1 (ATX1) activity, which catalyses H3K4 methylation and counteracts H3K27me3 repression (Alvarez-Venegas et al., 2003; Saleh et al., 2007), H3K4me3 levels in the MMCs were unaffected (supplementary material Fig. S4), suggesting the involvement of other SET-domain enzymes of redundant function with ATX1 (Thorstensen et al., 2011).

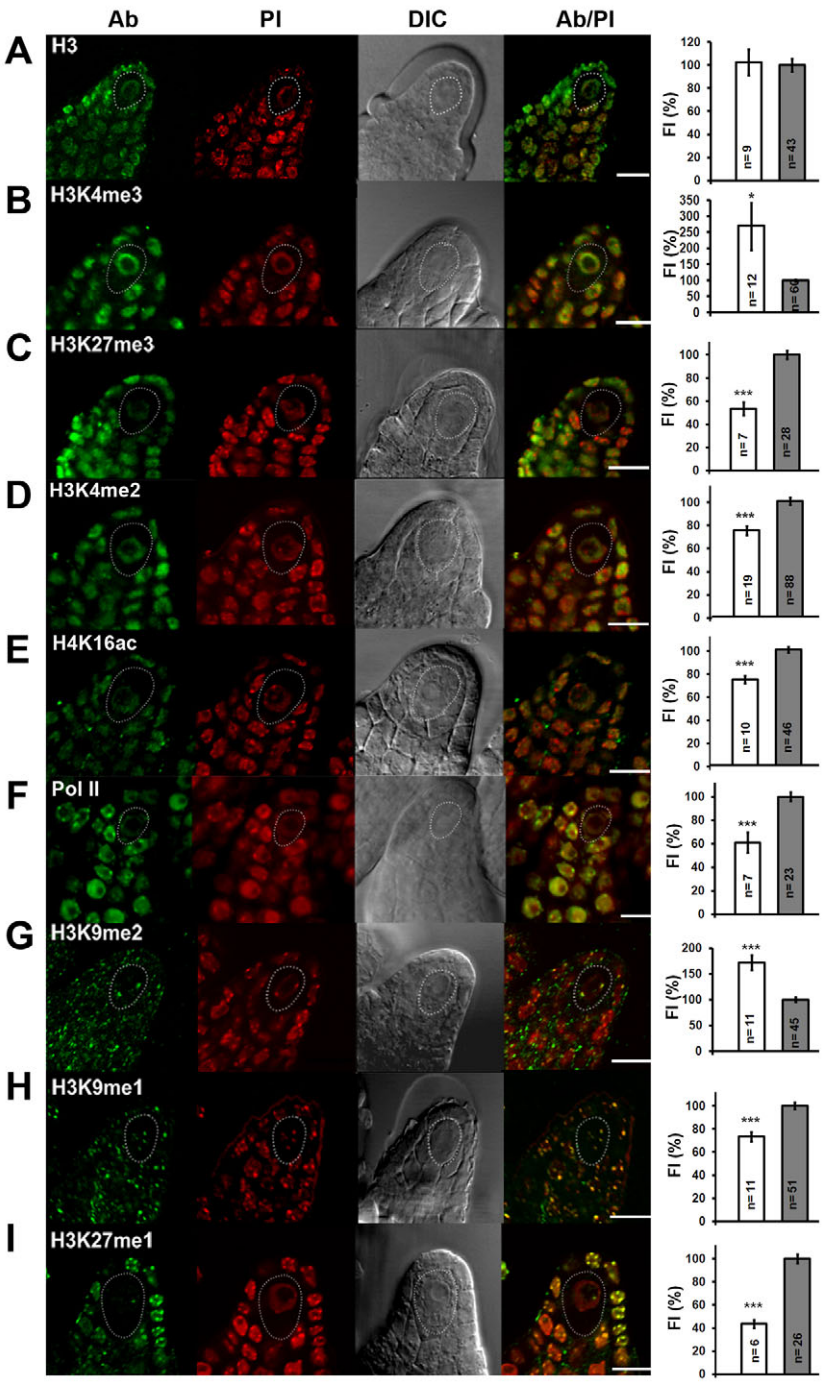

Fig. 3. The chromatin of the MMC is epigenetically distinct from that of the surrounding nucellar cells. (**A-I**) Global levels of H3 (A), modified H3 (B-D,G-I) and H4 (E) and active (Ser2 phosphorylated) PolII (F) were determined in the MMC and surrounding nucellar cells by whole-mount immunostaining in ovule primordia at stage 2-II. Representative images are shown for the antibody (Ab), DNA (propidium iodide, PI), transmitted light (DIC), and antibody signal overlaid with the DNA signal (Ab/PI). The relative fluorescence intensity in each channel was determined in 3D reconstructions in individual MMCs and nucellus nuclei. Bar charts show the average ratio Ab/PI relative to the nucellus (100%). White, MMC; gray, nucellus. The number of nuclei measured is indicated in each bar (*n*). Error bars indicate s.e.m. **P*<0.05, ****P*<0.001 (two-tailed Welch's *t*-test). Detailed quantifications at stage 2-II are provided in supplementary material Table S2 and the dynamics over the stages 1-II to 2-II are presented in supplementary material Fig. S5 and Table S3. Scale bars: 10 μm.

The histone marks found in MMCs are consistent with the establishment of a permissive chromatin environment. However, we also observed that the levels of H3K4me2 are reduced by 30% (Fig. 3D), as are the levels of H4K16ac, which correlates with active transcription (Tian et al., 2005; Jang et al., 2011; Vaquero-Sedas et al., 2011) (Fig. 3E). Furthermore, the presence of active RNA polymerase II (Ser2-phosphorylated RNA PolII) was significantly reduced (Fig. 3F), suggesting low transcriptional competence in the MMC.

Heterochromatin in the chromocenters of the *Arabidopsis* nucleus consists of centromeric and pericentromeric repeats, including transposons and rDNA sequences enriched in H3K9me1, H3K9me2, H3K27me1, H3K27me2, H4K20me1 and methylated DNA (Fransz et al., 2006). H3K9me2 is a hallmark of constitutive heterochromatin, yet is dispensable for its formation (Jasencakova et al., 2003). In dedifferentiated cells, such as protoplasts, or leaf cells lacking a DNA methylation maintenance function mediated by DECREASE IN DNA METHYLATION1 (DDM1), chromocenters are entirely disassembled whereby H3K9me2 immunostaining signals and centromeric repeats are redistributed (Jasencakova et al., 2003; Tessadori et al., 2007). In MMCs, by contrast, although the reduction in heterochromatin is comparable to that of dedifferentiated cells, H3K9me2 remained localized at conspicuous, although less numerous, chromocenters (Fig. 3G). This suggests that a fraction of sequences formerly associated with chromocenters were dispersed and lost H3K9me2

enrichment. Furthermore, the 1.6-fold enrichment of global H3K9me2 levels in MMC chromatin compared with nucellar cells suggests a reinforcement of heterochromatin silencing at sequences present in chromocenters. Increased H3K9me2 levels seem to occur at the expense of H3K9me1, which is present at reduced levels in MMC chromatin (Fig. 3H), possibly as a result of conversion to the dimethylated form by SUVR4 (Veiseth et al., 2011). Furthermore, the increase in H3K9me2 levels seems highly specific, as H3K27me1, another mark typically enriched at chromocenters, was almost absent from MMC heterochromatin at stage 2-II, with a 60% depletion relative to nucellar cells (Fig. 3I).

Clearly, MMC specification is accompanied by the establishment of a highly distinct chromatin configuration compared with that of the nucellus from which the MMC is derived. The MMC chromatin state is transcriptionally more permissive, yet has attenuated transcriptional competence. Also, it harbors a reduced heterochromatin fraction, yet is enriched in marks typical of silenced chromatin.

Reprogramming of chromatin modifications is gradual and partially synchronous with meiotic S phase, uncoupling heterochromatin and euchromatin replication

The chromatin state at stage 2-II is established gradually and asynchronously among histone modifications. Typically, H1 eviction precedes all other changes sequentially affecting heterochromatin and euchromatin, with the heterochromatic mark H3K9me2 increasing already at stage 1-II, whereas the euchromatic marks H3K27me3 and H3K4me3 change significantly only at later stages (2-II) (supplementary material Fig. S5, Table S3). To determine whether these distinct dynamics relate to a specific phase of the cell cycle (G1, S or G2), we characterized the meiotic S phase in the MMC. We quantified the DNA content in the MMC and compared it with that of three epidermal cells at the very tip of the nucellus (Fig. 4A; supplementary material Table S4). The DNA content progressively increased from stage 1-I to stage 2-II, indicating a slow genome replication occurring over several days. Consistent with this, *de novo* nucleotide incorporation, using EdU labeling (2-hour pulse), was observed as early as stage 1-I and lasted until stage 2-II (Fig. 4B,C). We also observed the continuous presence of a GFP-tagged variant of ORIGIN REPLICATION COMPLEX2 (ORC2-GFP) (Ngo et al., 2012) throughout meiotic S phase; this might indicate either progressive marking of early versus late replication origins or a role in establishing sister chromatid cohesion (MacAlpine et al., 2010) (Fig. 4D).

Thus, at the stage of H1 eviction (stage 1-I), the MMC has already engaged in DNA replication. However, the global loss of linker histones is unlikely to be a requirement for DNA replication as H1.1 remains detectable during the S phase of mitotic cell cycles (supplementary material Fig. S6). Interestingly, *de novo* EdU incorporation was predominantly found in heterochromatic chromocenters for MMCs at stage 1-I and 1-II, and in euchromatin for MMCs at stage 2-II (Fig. 4B,C; supplementary material Table S4). This suggests that the replication of cytologically detectable heterochromatin regions precedes that of most of the euchromatin during the meiotic S phase of female meiocytes in *Arabidopsis*. Furthermore, this observation raises the possibility that chromatin dynamics in heterochromatin (e.g. H3K9me2) and euchromatin (e.g. H3K27me3 and H3K4me3) might be coupled with the asynchronous replication of some heterochromatin and euchromatin regions, respectively.

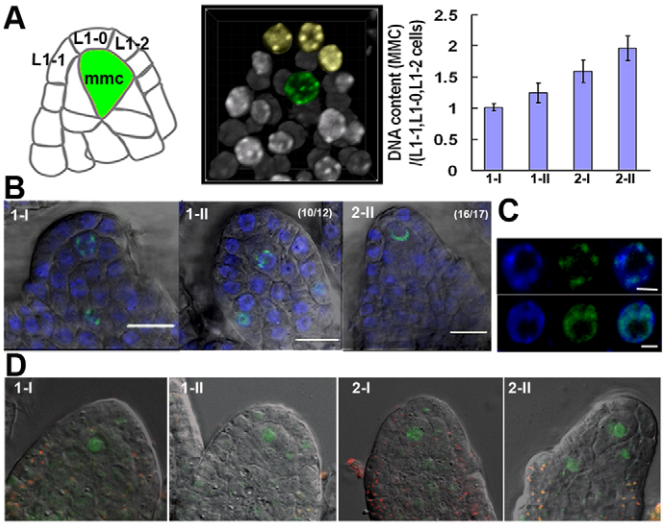

Fig. 4. A slow meiotic S phase in the MMC uncouples replication of heterochromatin and euchromatin. (**A**) Quantification of the DNA content in MMCs compared with that of the epidermal cells covering them (L1-1, L1-0, L1-2) indicates a progressive increase from G1 (stage 1-I) to G2 (stage 2-II) over several days. For each stage, *n*=10 MMCs and *n*=30 L1 cells. Bar chart shows the average ratio of DNA fluorescence intensity in MMC/nucellus; error bars indicate s.e.m. Detailed quantifications are given in supplementary material Table S4. (**B**,**C**) A 2-hour pulse of EdU incorporation reveals *de novo* DNA synthesis as early as stage 1-I predominantly in heterochromatin, and until stage 2-II when replication is essentially in euchromatin. The ratios (B) indicate the number of specific patterns/total observations: 10/12 primordia at stages 1-I and 1-II showed EdU signals enriched in heterochromatin foci; 16/17 primordia at stages 2-I and 2-II showed euchromatin signals. (C) A detailed view of the specific heterochromatin and euchromatin enrichment patterns in MMC nuclei at early (top) and late (bottom) stages. (**D**) Persistent nuclear localization of the ORC2 subunit (green) in MMCs throughout meiotic S phase. Scale bars: 10 µm.

Meiosis and selection of the functional megaspore entail additional and specific chromatin dynamics

Chromosome condensation marks the onset of the first meiotic prophase and is observed at stage 2-III of ovule development (Fig. 1). Consistent with their expected functions during chromosome condensation and segregation, respectively, the expression of H1.1 and H1.2 and of CENH3 is restored during meiosis (supplementary material Fig. S1). Furthermore, the increasing and decreasing trend of H3K9me2 and H3K27me3 signals, respectively, during MMC differentiation became more pronounced at prophase I, while H3K27me1 signals appeared stronger than at stage 2-II (supplementary material Fig. S7). Although the rapidly changing meiotic chromosomes render precise quantification difficult, meiosis clearly entails further changes in chromatin modifications.

Female meiosis produces four haploid spores, three of which degenerate while the surviving one, the functional megaspore (FMS), acquires a pluripotent fate; the FMS will form the multicellular gametophyte within which the gametes differentiate. To determine whether the chromatin state of the FMS resembles or differs from that of the MMC, we analyzed the same histone variants and modifications as above (Fig. 5; supplementary material Table S5, Figs S1, S8). Interestingly, the FMS chromatin

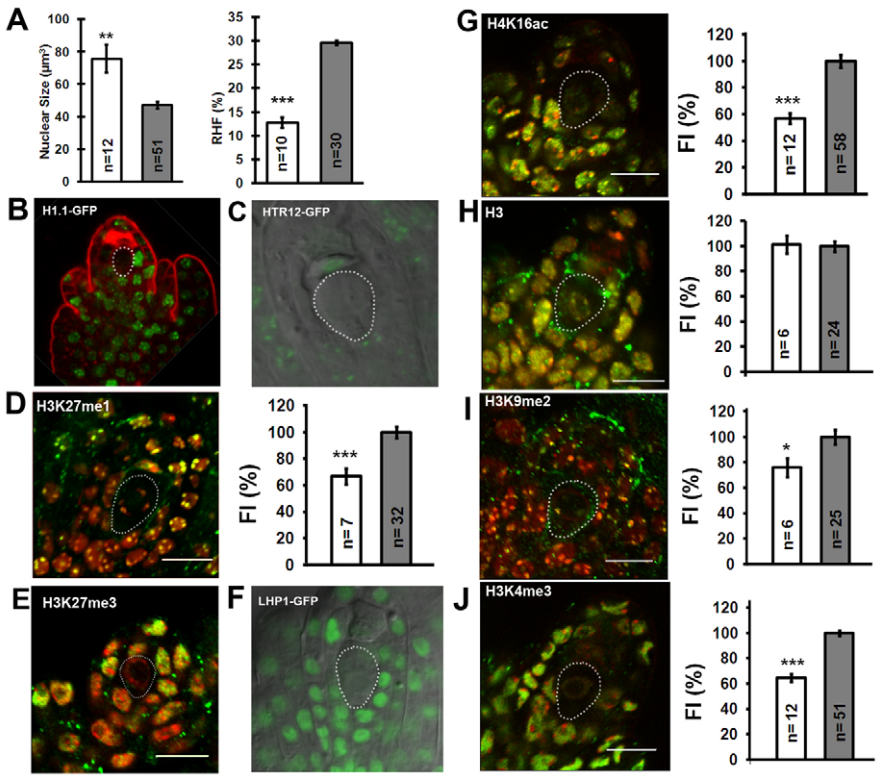

Fig. 5. Nuclear organization and chromatin state of the FMS resembles that of the MMC, but with specific hallmarks. (**A-J**) Nuclear organization and chromatin state of the FMS (the meiotic product giving rise to the embryo sac) was analyzed as for the MMC in Figs 1-3. The chromatin of the FMS largely recapitulates the state established in the MMC prior to meiosis, despite transient dynamic changes of some histone variants during meiosis (supplementary material Fig. S1). Exceptions are the histone modifications H3K9me2 and H3K4me3, which are decreased relative to the levels in the nucellus. The FMS is outlined. Error bars indicate s.e.m. **P*<0.05, ***P*<0.01, ****P*<0.001 (two-tailed Welch's *t*-test). Detailed quantifications are provided in supplementary material Table S5. Scale bars: 10 µm.

recapitulated the majority of characteristics observed in MMCs. This included decondensed chromatin, reduced heterochromatin content (Fig. 5A), a notable absence of H1.1 and H1.2 (Fig. 5B; supplementary material Fig. S1), undetectable levels of CENH3, strongly reduced levels of H3K27me1 (Fig. 5C,D), as well as undetectable levels of LHP1 and H3K27me3 (Fig. 5E,F). Similar to observations in the MMC, FMS chromatin shows low levels of H4K16ac (Fig. 5G) and active PolII, indicating low transcriptional activity, at least for the stage that we observed, just following FMS selection (supplementary material Fig. S8). At this stage, replication for subsequent gametogenesis has started (supplementary material Fig. S8). Furthermore, the detection of similar levels of H3 in the FMS and nucellar cells (Fig. 5H) confirmed that the decreased levels of immunostaining that we observed are not due to technical limitations. However, the FMS also exhibits specific, postmeiotic chromatin changes. The repressive mark H3K9me2 and the permissive mark H3K4me3, which were enriched in the MMC, were reduced in FMS chromatin compared with that of surrounding somatic cells (Fig. 5I,J).

Collectively, these results indicate that not only meiosis but also FMS selection entail additional chromatin reprogramming processes that follow both similar and specific trends compared with MMC differentiation.

Chromatin reprogramming in the MMC is likely to contribute to establishing competence for the postmeiotic fate

In wild-type *Arabidopsis* only one MMC is specified in the nucellus. The ARGONAUTE family member ARGONAUTE9 (AGO9) plays an essential role in restricting to a single MMC the number of reproductive lineage cells in each ovule via a small-RNA-dependent pathway. In the absence of AGO9, additional enlarged germline cells form ectopically and initiate the postmeiotic, gametophytic program (Olmedo-Monfil et al., 2010). To determine whether the chromatin dynamics that we observed in wild-type MMCs and FMSs are linked to the SRT, we looked at several chromatin markers in these supernumerary germline precursor cells. Similar to MMCs, the chromatin of these ectopic cells is devoid of H1.1 and H1.2 (Fig. 6A,B), whereas it retains HTR5 and HTR8 (Fig. 6C,D). The loss of both linker histone variants was confirmed in mutants affecting other components of this regulatory pathway [*suppressor of gene silencing3* (*sgs3*) and *rna-dependent rna polymerase6* (*rdr6*) mutants; supplementary material Fig. S9]. Furthermore, in *ago9* mutants, these supernumerary germline precursor cells also showed reduced levels of heterochromatic H3K27me1 (Fig. 6E; supplementary material Table S6), a hallmark of both the MMC and FMS chromatin state. Similarly, we also observed a drastic reduction of the euchromatic repressive modification H3K27me3 in these cells in a comparable manner to that in wild type (Fig. 6F; supplementary material Table S6). Because ectopic cells in *ago9* mutant ovule primordia do not initiate meiosis but instead directly differentiate into FMS (Olmedo-Monfil et al., 2010), these observations strongly support the idea that chromatin reprogramming constitutes a cell fate marker of the SRT.

We also analyzed mutant MMCs lacking the activity of SET DOMAIN GROUP2 (SDG2), one of several enzymes responsible for H3K4me3 deposition in *Arabidopsis* (Berr et al., 2010; Guo et al., 2010). In homozygous mutants, ovules are sterile and germline development typically shows a postmeiotic arrest at the FMS stage (Berr et al., 2010). Yet, we have shown that global levels of H3K4me3 increase in the MMC whereas they decrease in the FMS, suggesting that SDG2 might function before, rather than after, meiosis. Consistent with this hypothesis, the relative enrichment of H3K4me3 levels in *sdg2* MMCs only reached 60% of that in the wild type (Fig. 6G; supplementary material Table S6). Incidentally, detectable H3K4me3 in *sdg2* mutant MMCs suggests the activity of other H3K4 methyltransferases encoded in the *Arabidopsis* genome (Thorstensen et al., 2011). We observed progressive chromosome

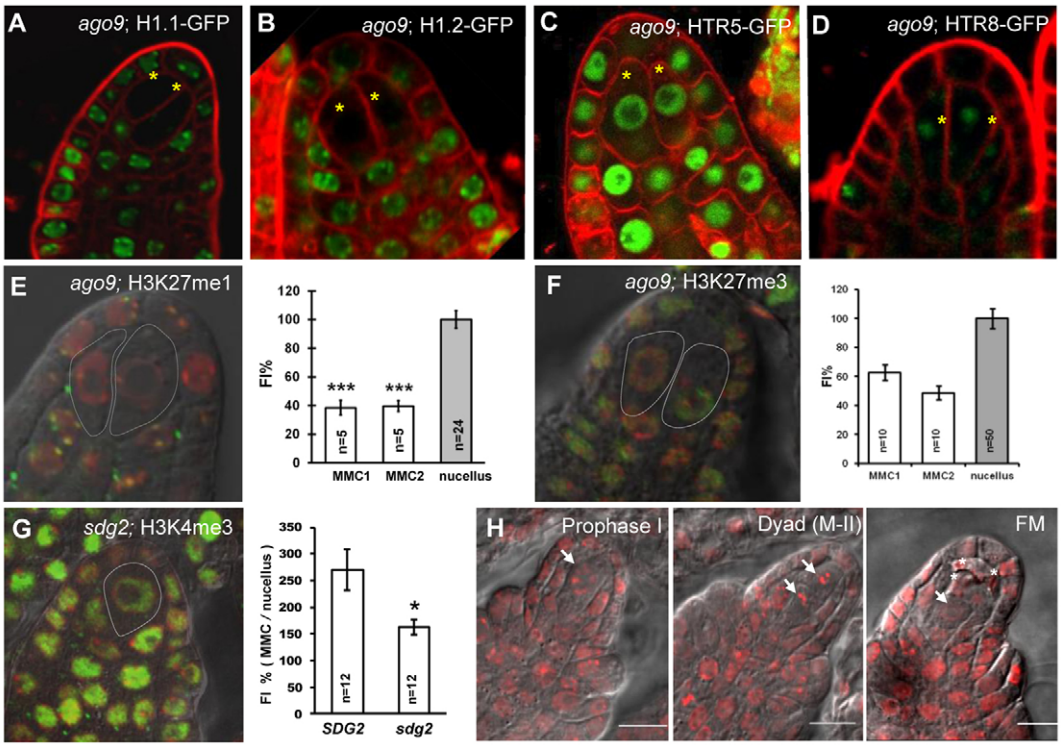

Fig. 6. Chromatin reprogramming in the MMC establishes competence for the postmeiotic developmental fate. (**A-F**) Ovule primordia lacking AGO9 activity show ectopic differentiation of germline precursor cells next to the MMC, expressing an ameiotic gametophyte developmental fate (Olmedo-Monfil et al., 2010). These cells recapitulate key events of chromatin reprogramming typical of MMCs: H1.1 and H1.2 depletion (A,B), expression of HTR5 and HTR8 variants (C,D), reduction of heterochromatin content and associated H3K27me1 (E) and reduction of the repressive euchromatic modification H3K27me3 (F). Quantifications as in Fig. 3. The analysis of H1.1-GFP in additional mutants of the AGO9 pathway are shown in supplementary material Fig. S9. (**G**,**H**) Ovule primordia lacking SDG2 activity show lower levels of H3K4me3 in the MMC relative to the nucellus, compared with in wild type. Yet this deficiency does not impair meiosis (H) (supplementary material Fig. S10), but compromises postmeiotic development (Berr et al., 2010). Error bars indicate s.e.m. *P<0.05, ***P<0.001 (two-tailed Welch's t-test). Detailed quantifications are given in supplementary material Table S6. Arrows in H indicate the MMC in prophase I, the two cells at the dyad stage and the four cells of the tetrad with FMS; asterisks indicate degenerated spores. Scale bars: 10 µm.

condensation at prophase I, as well as dyads and tetrads in *sdg2* developing ovules, suggesting that the substantial reduction in global H3K4me3 in *sdg2* MMCs did not affect meiosis (Fig. 6H; supplementary material Fig. S10) but rather prevented the FMS from initiating postmeiotic development (Berr et al., 2010) (our observations, not shown).

Altogether, our analyses of two antagonist mutants that ectopically express (*ago9*) or, by contrast, are impaired (*sdg2*) in the female gametophyte fate indicate that chromatin reprogramming is linked to, and is likely to contribute to, the acquisition of competence for the postmeiotic development of the female germline.

DISCUSSION

The data reported here suggest that, in the *Arabidopsis* ovule, the SRT is marked by extensive nuclear reorganization with drastic changes in chromatin condensation, composition and histone modification, including heterochromatin content and distribution. Analyses of mutants affecting megaspore differentiation indicate that these events contribute to establishing competence for the postmeiotic, gametophyte fate. The data reported here suggest that, in the *Arabidopsis* ovule, the SRT is marked by extensive nuclear reorganization with drastic changes in chromatin condensation, composition and histone modification, including heterochromatin content and distribution (Fig. S11).

Mechanisms of chromatin reprogramming

Chromatin reprogramming in the MMC is gradual and occurs in two consecutive phases characterized by: (1) early and rapid events including H1 and H2A.Z eviction, CENH3 turnover, increased levels of H3K9me2; and (2) late changes including decreased levels of H3K27me1, H3K9me1, H3K27me3, LHP1, H4Kac16 and PolII activity, while H3K4me3 levels increase. Interestingly, these two phases take place during a long meiotic S phase, during which we found a preferential replication of heterochromatin at early S phase and preceding that of euchromatin. Although late heterochromatin replication has been reported in male meiocytes of other plant species (Holm, 1977; Greer et al., 2012; Higgins et al., 2012), early replication is not uncommon and was found in male mammalian meiocytes (Latos-Bielenska and Vogel, 1992) or during animals mitosis [(Kim et al., 2003) and references therein].

The two phases of chromatin reprogramming might be partially coupled to the two phases of meiotic replication, raising the possibility of replication-dependent processes. For instance, the *de novo* incorporation of non-modified histones might partially contribute to the reduced H3K27me3:DNA signal ratio (supplementary material Fig. S4). However, the decreased absolute levels of H3K27me3 signal also implicate active demethylation. Yet a loss-of-function mutation in *REF6*, which encodes the major H3K27me3 demethylase (Lu et al., 2011), did not affect this process

(supplementary material Fig. S4), suggesting the involvement of as yet unknown alternative enzymes.

Increased levels of H3K9me3 at early stages of MMC differentiation are also likely to involve histone methyltransferase activity recruited at early S phase. When we examined mutants lacking SUVAR3-9 HOMOLOG4 (KRYPTONITE) activity (Lindroth et al., 2004), we found no cytologically detectable levels of H3K9me2 in ovule primordia (n=24; supplementary material Fig. S4), as has been reported for mature ovules (Autran et al., 2011). However, these mutants exhibit normal fertility, suggesting the involvement of factors that act redundantly with H3K9me2 in heterochromatin silencing (Thorstensen et al., 2011).

H4K3me3 chromatin modification is catalysed by several enzymes, including *Arabidopsis* ATX1 and SDG2, as well as other potentially active SET or ATRX proteins (Alvarez-Venegas and Avramova, 2002). Whereas we found no changes in H3K4me3 levels in *atx1* mutant primordia (supplementary material Fig. S4), SDG2 contributed to H3K4me3 dynamics in the MMC (Fig. 6 and discussed below).

Finally, genome-wide eviction of H1 and H2A.Z histone variants occurs prior to euchromatin replication, suggesting an active, replication-independent process, yet possibly coordinated by cell cycle regulators. In animals, CDK2-mediated phosphorylation of histone H1 during the mitotic S phase destabilizes H1-chromatin interactions resulting in a more open chromatin structure (Contreras et al., 2003). A similar process is likely to be in place in plants, whereas a CDK2 type of activity could possibly contribute to H1 phosphorylation in wheat male meiocytes (Greer et al., 2012). In addition, H1 binding is modulated by the histone chaperone NUCLEOSOME ASSEMBLY PROTEIN 1 (NAP1) (Kepert et al., 2005). *Arabidopsis* plants lacking NAP1;1-3 activity [triple mutant (Liu et al., 2009)] or the activity of the NAP1-related proteins NRP1 and NRP2 [double mutant (Zhu et al., 2006)] show normal eviction of both H1.1 and H1.2 in the MMC and reincorporation at meiosis (supplementary material Fig. S4). Clearly, however, a proteasome-mediated degradation process appears to contribute to eliminate (probably unbound) H1 from the MMC chromatin (Fig. 2; supplementary material Fig. S3). Further investigations are thus required to identify the factors controlling H1 dynamics in the MMC, a precocious event that is likely to be crucial for epigenetic reprogramming (see below).

Chromatin reprogramming in the MMC and meiosis

The SRT is intimately linked with the transition from a mitotic to a meiotic cell cycle program. Chromatin reprogramming in the MMC could thus potentially serve several meiotic functions: in regulating entry to the meiotic cell cycle, in meiotic progression, or both.

A few reproductive mutants in maize and *Arabidopsis* initiate SMC differentiation but fail to enter meiosis and produce non-reproductive mitotic cells (Pawlowski et al., 2007), showing that SMC specification can be uncoupled from the meiotic program. In the budding yeast *Saccharomyces cerevisiae*, depletion of the linker histone Hho1 is a prerequisite to instruct entry to meiosis through derepression of meiotic genes (Bryant et al., 2012). H1 depletion in the MMC occurs as early as stage 1-I of ovule primordia development, coinciding with the onset of the meiotic S phase. This event could thus contribute to instructing entry into meiosis in MMCs. However, H1 depletion is likely to have additional functions because ectopic *ago9* MMCs also undergo this event yet avoid meiosis and initiate gametophyte development instead (Olmedo-Monfil et al., 2010).

The meiotic cell cycle is initiated at interphase, during which a typically long S phase takes place in most organisms studied so far, and deserves preparatory functions to meiotic execution (Bennett, 1977). The end of DNA replication entails the establishment of sister chromatid cohesion, a prerequisite for homologous chromosome pairing and synapsis enabling meiotic recombination during prophase I (Osman et al., 2011). It was recently suggested that H1 destabilization upon CDK2-mediated phosphorylation during the meiotic S phase might contribute to heterochromatin decondensation, facilitating, in turn, sister chromatid cohesion in wheat male meiocytes (Greer et al., 2012). In addition, perturbation of H1 stoichiometry in tobacco flowers induced aberrant male meiosis involving incorrect chromosome pairing and segregation (Prymakowska-Bosak et al., 1999). Thus, H1 dynamics in *Arabidopsis* MMCs committed to meiosis (depletion at early S phase and reloading at early prophase I) might reflect similar roles. Furthermore, additional chromatin modifiers are essential to the execution of meiotic events following meiotic S phase (Tiang et al., 2012). For instance, DNA methylation and histone H4 acetylation events contribute to chiasma distribution and frequency in *Arabidopsis* (Perrella et al., 2010; Yelina et al., 2012). Whether H3K9 and H3K4 methylation also contribute to the formation and repair of double-strand breaks, which underlies genetic recombination, in plant as in animal meiosis (Ivanovska and Orr-Weaver, 2006; Borde et al., 2009) remains to be determined. A speculative role for chromatin reprogramming in the MMC could thus lie in the establishment of an epigenetic landscape that is instructive for further chromatin dynamics and subsequent meiotic events (Tiang et al., 2012).

Chromatin reprogramming and epigenetic resetting

Besides the possible contribution to meiotic execution mentioned above, chromatin reprogramming clearly plays a role in establishing the postmeiotic, gametophyte fate. This conclusion is based on the analysis of two antagonistic mutants in which gametophyte development is either ectopically expressed and meiosis is avoided (*ago9*) or is impaired while meiosis progresses apparently normally (*sdg2*). We thus propose that chromatin reprogramming underlies a process of epigenetic reprogramming.

From a developmental perspective, SMCs are the functional equivalent of animal PGCs. During development, PGCs undergo a genome-wide and complex chromatin reprogramming, including nuclear size increase, loss of heterochromatic chromocenters, depletion of somatic linker histones and chromatin decondensation, redistribution of HP1, reduction in H3K9me2, H3K9ac and H3K27me3 and histone replacements (Hajkova et al., 2008; Seki et al., 2005; Mansour et al., 2012). These events take place during a proliferative phase of PGCs and part of the chromatin dynamics may be coupled with the cell-cycle stage (Kagiwada et al., 2012). Interestingly, chromatin dynamics in MMCs share many features with that of animal PGCs. Epigenetic reprogramming in PGCs has multiple roles, including preparation for meiosis, erasure of imprints and epimutations, and the removal of epigenetic barriers to pluripotency, thereby resetting the ‘ground state’ of the epigenome (Hajkova, 2011; Hackett et al., 2012). In particular, H3K27me3 demethylation, H1 depletion and DNA demethylation are crucial for enabling pluripotency (Terme et al., 2011; Hackett et al., 2012; Mansour et al., 2012). Similarly, H3K27me3 reprogramming, chromatin decondensation and reduction in H1 and LHP1 are considered as hallmarks of plant cell dedifferentiation towards pluripotency (Zhao et al., 2001; Williams et al., 2003; Tessadori et

al., 2007; Alatzas et al., 2008; He et al., 2012). The analysis of *ago9* ectopic germline precursor cells, which exhibit an ameiotic, gametophyte fate, further indicate that H1 depletion as well as H3K27me3 reduction in the MMC contribute to establishing a gametophyte fate, which also involves pluripotent development. Further evidence for this hypothesis is provided by the overexpression of H1 genes in the nucellus of maize hybrids developing ameiotic, unreduced gametophytes (Garcia-Aguilar et al., 2010). Moreover, the analysis of plants lacking SDG2 activity uncovered a postmeiotic role for H3K4me3 deposition in the MMC. In *sdg2* MMCs, H3K4 methylation is not fully compromised and meiotic progression appears normal at the cytological level, yet FMSs are not competent to resume gametophyte development (Berr et al., 2010) (our observations). Thus, we propose that reprogramming of the H3K4me3 landscape at the end of the meiotic S phase contributes to the transcriptional activation of genes relevant for the pluripotent development of the female gametophyte. Consistent with this hypothesis, the MMC transcriptome was found to express genes involved in gametophyte but also in early embryo development, suggesting potential long-term relevance of reprogramming events in the MMC (Schmidt et al., 2011).

The accepted view is that DNA methylation patterns are relatively stable during plant reproduction (Jullien and Berger, 2010), allowing for transgenerational inheritance of epigenetic states (Paszkowski and Grossniklaus, 2011; Saze, 2012). However, H1 stoichiometry in the plant nucleus, besides its impact on the structural organization of chromatin, is likely to influence DNA methylation patterns as it does in both plant and animal somatic cells (Fan et al., 2005; Wierzbicki and Jerzmanowski, 2005; Yang et al., 2013; Zemach et al., 2013). H2A.Z depletion in the MMC further increases the potential for reprogramming of DNA methylation because these two marks are mutually exclusive (Zilberman, 2008). Profiling of methylated sites in different contexts (CG, CHG and CHH) (Vaillant and Paszkowski, 2007) will be required to resolve the extent to which H1 and H2A.Z dynamics influence DNA methylation patterns during MMC specification. How this global reprogramming event would be compatible with the transgenerational inheritance of epigenetic states remains to be determined (Paszkowski and Grossniklaus, 2011; Saze, 2012). However, the tools necessary for such investigations are not currently available: single-cell epigenome profiling in MMCs is hindered by the high cellular dilution of MMCs within floral tissues (Wuest et al., 2013), and cytogenetic mapping of DNA methylation provides insufficient resolution with signals preferentially located at the periphery of centromeres (Fransz et al., 2006; Zhang et al., 2008) and does not resolve the sequence context of DNA methylation.

Although further technological improvements and investigations are required to disentangle the short- and long-term developmental impact of the different events affecting the MMC epigenome, we propose that global chromatin decondensation and H1 eviction in MMCs might allow an initial relaxation of the chromatin structure that is compatible with large-scale reprogramming of H3K27me3 and H3K4me3 patterns and possibly also DNA methylation. Collectively, these events are likely to contribute to establishing competence for the pluripotent, postmeiotic fate in the female gametophyte. Epigenome profiling in the MMC remains the next challenge to further define these reprogramming events.

Acknowledgements
We thank Ueli Grossniklaus (University of Zürich, Switzerland) for insightful discussions, technical and financial support and critical reading of the manuscript; Mathieu Ingouff (University of Montpellier, France), Phillip Wigge (Sainsbury Institute, Cambridge, UK), Jean-Philippe Vielle-Calzada (LANGEBIO, Mexico), Koji Goto (Research Institute for Biological Sciences, Okayama, Japan), WenHui Shen and Alexandre Berr (IBMP Strasbourg, France), Xia Cui and Xiaofeng Cao (Chinese Academy of Sciences, China) for providing seeds; Robert Dudler (University of Zürich, Switzerland) for providing Syringolin A; and Valeria Gagliardini, Christof Eichenberger, Arturo Bolanos and Peter Kopf for general lab support.

Funding
This research was funded by the University of Zürich; grants from the Swiss National Foundation to C.B. [31003A_130722] and Ueli Grossniklaus [31003A_141245 and 31003AB-126006]; the National Science Center to K.R. [2011/01/N/NZ3/05362]; the European Cooperation in Science and Technology [MNiSW 312/N-COST/2008/0] to M.P., K.R. and A.J.; and the Agence Nationale de la Recherche to D.G. [Programme ANR-BLANC-2012].

Competing interests statement
The authors declare no competing financial interests.

Author contributions
The experiments were designed by W.S., D.G., K.R., A.J. and C.B., and carried out by W.S., D.G., K.R., M.W., M.P., M.K. and C.B. W.S., D.G., K.R., A.J. and C.B. wrote the manuscript.

Supplementary material
Supplementary material available online at
http://dev.biologists.org/lookup/suppl/doi:10.1242/dev.095034/-/DC1

References
Ahmad, K. and Henikoff, S. (2002). Histone H3 variants specify modes of chromatin assembly. *Proc. Natl. Acad. Sci. USA* **99 Suppl. 4**, 16477-16484.
Alatzas, A., Srebreva, L. and Foundouli, A. (2008). Distribution of linker histone variants during plant cell differentiation in the developmental zones of the maize root, dedifferentiation in callus culture after auxin treatment. *Biol. Res.* **41**, 205-215.
Alvarez-Venegas, R. and Avramova, Z. (2002). SET-domain proteins of the Su(var)3-9, E(z) and trithorax families. *Gene* **285**, 25-37.
Alvarez-Venegas, R., Pien, S., Sadder, M., Witmer, X., Grossniklaus, U. and Avramova, Z. (2003). ATX-1, an Arabidopsis homolog of trithorax, activates flower homeotic genes. *Curr. Biol.* **13**, 627-637.
Armstrong, S. J. and Jones, G. H. (2003). Meiotic cytology and chromosome behaviour in wild-type Arabidopsis thaliana. *J. Exp. Bot.* **54**, 1-10.
Ascenzi, R. and Gantt, J. S. (1997). A drought-stress-inducible histone gene in Arabidopsis thaliana is a member of a distinct class of plant linker histone variants. *Plant Mol. Biol.* **34**, 629-641.
Autran, D., Baroux, C., Raissig, M. T., Lenormand, T., Wittig, M., Grob, S., Steimer, A., Barann, M., Klostermeier, U. C., Leblanc, O. et al. (2011). Maternal epigenetic pathways control parental contributions to Arabidopsis early embryogenesis. *Cell* **145**, 707-719.
Baroux, C., Pecinka, A., Fuchs, J., Schubert, I. and Grossniklaus, U. (2007). The triploid endosperm genome of Arabidopsis adopts a peculiar, parental-dosage-dependent chromatin organization. *Plant Cell* **19**, 1782-1794.
Bendel-Stenzel, M., Anderson, R., Heasman, J. and Wylie, C. (1998). The origin and migration of primordial germ cells in the mouse. *Semin. Cell Dev. Biol.* **9**, 393-400.
Bennett, M. D. (1977). The time and duration of meiosis. *Philos. Trans. R. Soc. B* **277**, 201-226.
Berger, F. and Twell, D. (2011). Germline specification and function in plants. *Annu. Rev. Plant Biol.* **62**, 461-484.
Berr, A., McCallum, E. J., Ménard, R., Meyer, D., Fuchs, J., Dong, A. and Shen, W. H. (2010). Arabidopsis SET DOMAIN GROUP2 is required for H3K4 trimethylation and is crucial for both sporophyte and gametophyte development. *Plant Cell* **22**, 3232-3248.
Borde, V., Robine, N., Lin, W., Bonfils, S., Géli, V. and Nicolas, A. (2009). Histone H3 lysine 4 trimethylation marks meiotic recombination initiation sites. *EMBO J.* **28**, 99-111.
Bryant, J. M., Govin, J., Zhang, L., Donahue, G., Pugh, B. F. and Berger, S. L. (2012). The linker histone plays a dual role during gametogenesis in Saccharomyces cerevisiae. *Mol. Cell. Biol.* **32**, 2771-2783.
Calarco, J. P. and Martienssen, R. A. (2011). Genome reprogramming and small interfering RNA in the Arabidopsis germline. *Curr. Opin. Genet. Dev.* **21**, 134-139.
Coleman-Derr, D. and Zilberman, D. (2012). Deposition of histone variant H2A.Z within gene bodies regulates responsive genes. *PLoS Genet.* **8**, e1002988.
Contreras, A., Hale, T. K., Stenoien, D. L., Rosen, J. M., Mancini, M. A. and Herrera, R. E. (2003). The dynamic mobility of histone H1 is regulated by cyclin/CDK phosphorylation. *Mol. Cell. Biol.* **23**, 8626-8636.

Cooper, D. C. (1937). Macrosporogenesis and embryo-sac development in euchlaena mexicana and zea mays. *J. Agric. Res.* **55**, 539-551.
Deal, R. B. and Henikoff, S. (2010). Gene regulation: a chromatin thermostat. *Nature* **463**, 887-888.
Fan, Y., Nikitina, T., Zhao, J., Fleury, T. J., Bhattacharyya, R., Bouhassira, E. E., Stein, A., Woodcock, C. L. and Skoultchi, A. I. (2005). Histone H1 depletion in mammals alters global chromatin structure but causes specific changes in gene regulation. *Cell* **123**, 1199-1212.
Fang, Y. and Spector, D. L. (2005). Centromere positioning and dynamics in living Arabidopsis plants. *Mol. Biol. Cell* **16**, 5710-5718.
Fransz, P., ten Hoopen, R. and Tessadori, F. (2006). Composition and formation of heterochromatin in Arabidopsis thaliana. *Chromosome Res.* **14**, 71-82.
Fuchs, J., Demidov, D., Houben, A. and Schubert, I. (2006). Chromosomal histone modification patterns – from conservation to diversity. *Trends Plant Sci.* **11**, 199-208.
Garcia-Aguilar, M., Michaud, C., Leblanc, O. and Grimanelli, D. (2010). Inactivation of a DNA methylation pathway in maize reproductive organs results in apomixis-like phenotypes. *Plant Cell* **22**, 3249-3267.
Grant-Downton, R. T. and Dickinson, H. G. (2006). Epigenetics and its implications for plant biology 2. The epigenetic epiphany: epigenetics, evolution and beyond. *Ann. Bot. (Lond.)* **97**, 11-27.
Greer, E., Martín, A. C., Pendle, A., Colas, I., Jones, A. M., Moore, G. and Shaw, P. (2012). The Ph1 locus suppresses Cdk2-type activity during premeiosis and meiosis in wheat. *Plant Cell* **24**, 152-162.
Groll, M., Schellenberg, B., Bachmann, A. S., Archer, C. R., Huber, R., Powell, T. K., Lindow, S., Kaiser, M. and Dudler, R. (2008). A plant pathogen virulence factor inhibits the eukaryotic proteasome by a novel mechanism. *Nature* **452**, 755-758.
Guo, L., Yu, Y., Law, J. A. and Zhang, X. (2010). SET DOMAIN GROUP2 is the major histone H3 lysine 4 trimethyltransferase in Arabidopsis. *Proc. Natl. Acad. Sci. USA* **107**, 18557-18562.
Hackett, J. A., Zylicz, J. J. and Surani, M. A. (2012). Parallel mechanisms of epigenetic reprogramming in the germline. *Trends Genet.* **28**, 164-174.
Hajkova, P. (2011). Epigenetic reprogramming in the germline: towards the ground state of the epigenome. *Philos. Trans. R. Soc. B* **366**, 2266-2273.
Hajkova, P., Ancelin, K., Waldmann, T., Lacoste, N., Lange, U. C., Cesari, F., Lee, C., Almouzni, G., Schneider, R. and Surani, M. A. (2008). Chromatin dynamics during epigenetic reprogramming in the mouse germ line. *Nature* **452**, 877-881.
He, C., Chen, X., Huang, H. and Xu, L. (2012). Reprogramming of H3K27me3 is critical for acquisition of pluripotency from cultured Arabidopsis tissues. *PLoS Genet.* **8**, e1002911.
Hellens, R. P., Edwards, E. A., Leyland, N. R., Bean, S. and Mullineaux, P. M. (2000). pGreen: a versatile and flexible binary Ti vector for Agrobacterium-mediated plant transformation. *Plant Mol. Biol.* **42**, 819-832.
Higgins, J. D., Perry, R. M., Barakate, A., Ramsay, L., Waugh, R., Halpin, C., Armstrong, S. J. and Franklin, F. C. (2012). Spatiotemporal asymmetry of the meiotic program underlies the predominantly distal distribution of meiotic crossovers in barley. *Plant Cell* **24**, 4096-4109.
Holm, P. B. (1977). The premeiotic DNA replication of euchromatin and heterochromatin in Lilium longiflorum (Thunb.). *Carlsberg Res. Commun.* **42**, 249-281.
Houben, A., Kumke, K., Nagaki, K. and Hause, G. (2011). CENH3 distribution and differential chromatin modifications during pollen development in rye (Secale cereale L.). *Chromosome Res.* **19**, 471-480.
Ibarra, C. A., Feng, X., Schoft, V. K., Hsieh, T. F., Uzawa, R., Rodrigues, J. A., Zemach, A., Chumak, N., Machlicova, A., Nishimura, T. et al. (2012). Active DNA demethylation in plant companion cells reinforces transposon methylation in gametes. *Science* **337**, 1360-1364.
Ingouff, M., Hamamura, Y., Gourgues, M., Higashiyama, T. and Berger, F. (2007). Distinct dynamics of HISTONE3 variants between the two fertilization products in plants. *Curr. Biol.* **17**, 1032-1037.
Ingouff, M., Rademacher, S., Holec, S., Soljić, L., Xin, N., Readshaw, A., Foo, S. H., Lahouze, B., Sprunck, S. and Berger, F. (2010). Zygotic resetting of the HISTONE 3 variant repertoire participates in epigenetic reprogramming in Arabidopsis. *Curr. Biol.* **20**, 2137-2143.
Ivanovska, I. and Orr-Weaver, T. L. (2006). Histone modifications and the chromatin scaffold for meiotic chromosome architecture. *Cell Cycle* **5**, 2064-2071.
Jang, I. C., Chung, P. J., Hemmes, H., Jung, C. and Chua, N. H. (2011). Rapid and reversible light-mediated chromatin modifications of Arabidopsis phytochrome A locus. *Plant Cell* **23**, 459-470.
Jasencakova, Z., Soppe, W. J., Meister, A., Gernand, D., Turner, B. M. and Schubert, I. (2003). Histone modifications in Arabidopsis – high methylation of H3 lysine 9 is dispensable for constitutive heterochromatin. *Plant J.* **33**, 471-480.
Jullien, P. E. and Berger, F. (2010). DNA methylation reprogramming during plant sexual reproduction? *Trends Genet.* **26**, 394-399.
Jullien, P. E., Susaki, D., Yelagandula, R., Higashiyama, T. and Berger, F. (2012). DNA methylation dynamics during sexual reproduction in Arabidopsis thaliana. *Curr. Biol.* **22**, 1825-1830.
Kagiwada, S., Kurimoto, K., Hirota, T., Yamaji, M. and Saitou, M. (2012). Replication-coupled passive DNA demethylation for the erasure of genome imprints in mice. *EMBO J.* **32**, 340-353.
Kepert, J. F., Mazurkiewicz, J., Heuvelman, G. L., Tóth, K. F. and Rippe, K. (2005). NAP1 modulates binding of linker histone H1 to chromatin and induces an extended chromatin fiber conformation. *J. Biol. Chem.* **280**, 34063-34072.
Kim, S. M., Dubey, D. D. and Huberman, J. A. (2003). Early-replicating heterochromatin. *Genes Dev.* **17**, 330-335.
Kotogany, E., Dudits, D., Horvath, G. V. and Ayaydin, F. (2010). A rapid and robust assay for detection of S-phase cell cycle progression in plant cells and tissues by using ethynyl deoxyuridine. *Plant Methods* **6**, 5.
Kumar, S. V. and Wigge, P. A. (2010). H2A.Z-containing nucleosomes mediate the thermosensory response in Arabidopsis. *Cell* **140**, 136-147.
Latos-Bielenska, A. and Vogel, W. (1992). Demonstration of replication patterns in the last premeiotic S-phase of male Chinese hamsters after BrdU pulse labeling. *Chromosoma* **101**, 279-283.
Libault, M., Tessadori, F., Germann, S., Snijder, B., Fransz, P. and Gaudin, V. (2005). The Arabidopsis LHP1 protein is a component of euchromatin. *Planta* **222**, 910-925.
Lindroth, A. M., Shultis, D., Jasencakova, Z., Fuchs, J., Johnson, L., Schubert, D., Patnaik, D., Pradhan, S., Goodrich, J., Schubert, I. et al. (2004). Dual histone H3 methylation marks at lysines 9 and 27 required for interaction with CHROMOMETHYLASE3. *EMBO J.* **23**, 4286-4296.
Liu, Z., Zhu, Y., Gao, J., Yu, F., Dong, A. and Shen, W. H. (2009). Molecular and reverse genetic characterization of NUCLEOSOME ASSEMBLY PROTEIN1 (NAP1) genes unravels their function in transcription and nucleotide excision repair in Arabidopsis thaliana. *Plant J.* **59**, 27-38.
Lu, F., Cui, X., Zhang, S., Jenuwein, T. and Cao, X. (2011). Arabidopsis REF6 is a histone H3 lysine 27 demethylase. *Nat. Genet.* **43**, 715-719.
MacAlpine, H. K., Gordân, R., Powell, S. K., Hartemink, A. J. and MacAlpine, D. M. (2010). Drosophila ORC localizes to open chromatin and marks sites of cohesin complex loading. *Genome Res.* **20**, 201-211.
Maheshwari, P. (1950) *An Introduction to The Embryology of Angiosperms*. New York, NY: McGraw-Hill.
Maison, C. and Almouzni, G. (2004). HP1 and the dynamics of heterochromatin maintenance. *Nat. Rev. Mol. Cell Biol.* **5**, 296-304.
Mansour, A. A., Gafni, O., Weinberger, L., Zviran, A., Ayyash, M., Rais, Y., Krupalnik, V., Zerbib, M., Amann-Zalcenstein, D., Maza, I. et al. (2012). The H3K27 demethylase Utx regulates somatic and germ cell epigenetic reprogramming. *Nature* **488**, 409-413.
Messing, J. and Grossniklaus, U. (1999). Genomic imprinting in plants. *Results Probl. Cell Differ.* **25**, 23-40.
Mito, Y., Henikoff, J. G. and Henikoff, S. (2005). Genome-scale profiling of histone H3.3 replacement patterns. *Nat. Genet.* **37**, 1090-1097.
Nakahigashi, K., Jasencakova, Z., Schubert, I. and Goto, K. (2005). The Arabidopsis heterochromatin protein1 homolog (TERMINAL FLOWER2) silences genes within the euchromatic region but not genes positioned in heterochromatin. *Plant Cell Physiol.* **46**, 1747-1756.
Ngo, Q. A., Baroux, C., Guthörl, D., Mozerov, P., Collinge, M. A., Sundaresan, V. and Grossniklaus, U. (2012). The Armadillo repeat gene ZAK IXIK promotes Arabidopsis early embryo and endosperm development through a distinctive gametophytic maternal effect. *Plant Cell* **24**, 4026-4043.
Olmedo-Monfil, V., Durán-Figueroa, N., Arteaga-Vázquez, M., Demesa-Arévalo, E., Autran, D., Grimanelli, D., Slotkin, R. K., Martienssen, R. A. and Vielle-Calzada, J.-P. (2010). Control of female gamete formation by a small RNA pathway in Arabidopsis. *Nature* **464**, 628-632.
Osman, K., Higgins, J. D., Sanchez-Moran, E., Armstrong, S. J. and Franklin, F. C. (2011). Pathways to meiotic recombination in Arabidopsis thaliana. *New Phytol.* **190**, 523-544.
Paszkowski, J. and Grossniklaus, U. (2011). Selected aspects of transgenerational epigenetic inheritance and resetting in plants. *Curr. Opin. Plant Biol.* **14**, 195-203.
Pawlowski, W. P., Sheehan, M. J. and Ronceret, A. (2007). In the beginning: the initiation of meiosis. *BioEssays* **29**, 511-514.
Perrella, G., Consiglio, M. F., Aiese-Cigliano, R., Cremona, G., Sanchez-Moran, E., Barra, L., Errico, A., Bressan, R. A., Franklin, F. C. and Conicella, C. (2010). Histone hyperacetylation affects meiotic recombination and chromosome segregation in Arabidopsis. *Plant J.* **62**, 796-806.
Pillot, M., Baroux, C., Vazquez, M. A., Autran, D., Leblanc, O., Vielle-Calzada, J. P., Grossniklaus, U. and Grimanelli, D. (2010). Embryo and endosperm inherit distinct chromatin and transcriptional states from the female gametes in Arabidopsis. *Plant Cell* **22**, 307-320.
Prymakowska-Bosak, M., Przewłoka, M. R., Slusarczyk, J., Kuraś, M., Lichota, J., Kiliańczyk, B. and Jerzmanowski, A. (1999). Linker histones play a role in male meiosis and the development of pollen grains in tobacco. *Plant Cell* **11**, 2317-2329.

Ravi, M., Shibata, F., Ramahi, J. S., Nagaki, K., Chen, C., Murata, M. and Chan, S. W. (2011). Meiosis-specific loading of the centromere-specific histone CENH3 in Arabidopsis thaliana. *PLoS Genet.* **7**, e1002121.
Robinson, P. J. and Rhodes, D. (2006). Structure of the '30 nm' chromatin fibre: a key role for the linker histone. *Curr. Opin. Struct. Biol.* **16**, 336-343.
Saleh, A., Al-Abdallat, A., Ndamukong, I., Alvarez-Venegas, R. and Avramova, Z. (2007). The Arabidopsis homologs of trithorax (ATX1) and enhancer of zeste (CLF) establish 'bivalent chromatin marks' at the silent AGAMOUS locus. *Nucleic Acids Res.* **35**, 6290-6296.
Saze, H. (2012). Transgenerational inheritance of induced changes in the epigenetic state of chromatin in plants. *Genes Genet. Syst.* **87**, 145-152.
Schmidt, A., Wuest, S. E., Vijverberg, K., Baroux, C., Kleen, D. and Grossniklaus, U. (2011). Transcriptome analysis of the Arabidopsis megaspore mother cell uncovers the importance of RNA helicases for plant germline development. *PLoS Biol.* **9**, e1001155.
Schneitz, K., Hülskamp, M. and Pruitt, R. E. (1995). Wild-type ovule development in Arabidopsis thaliana: a light microscope study of cleared whole-mount tissue. *Plant J.* **7**, 731-749.
Schoft, V. K., Chumak, N., Mosiolek, M., Slusarz, L., Komnenovic, V., Brownfield, L., Twell, D., Kakutani, T. and Tamaru, H. (2009). Induction of RNA-directed DNA methylation upon decondensation of constitutive heterochromatin. *EMBO Rep.* **10**, 1015-1021.
Schulz, P. and Jensen, W. A. (1981). Pre-fertilization in Capsella: ultrastructure and ultrachemical localization of acid phosphatase in female meiocytes. *Protoplasma* **107**, 27-45.
Seki, Y., Hayashi, K., Itoh, K., Mizugaki, M., Saitou, M. and Matsui, Y. (2005). Extensive and orderly reprogramming of genome-wide chromatin modifications associated with specification and early development of germ cells in mice. *Dev. Biol.* **278**, 440-458.
Shaner, N. C., Lin, M. Z., McKeown, M. R., Steinbach, P. A., Hazelwood, K. L., Davidson, M. W. and Tsien, R. Y. (2008). Improving the photostability of bright monomeric orange and red fluorescent proteins. *Nat. Methods* **5**, 545-551.
Singh, M., Goel, S., Meeley, R. B., Dantec, C., Parrinello, H., Michaud, C., Leblanc, O. and Grimanelli, D. (2011). Production of viable gametes without meiosis in maize deficient for an ARGONAUTE protein. *Plant Cell* **23**, 443-458.
Slotkin, R. K., Vaughn, M., Borges, F., Tanurdzić, M., Becker, J. D., Feijó, J. A. and Martienssen, R. A. (2009). Epigenetic reprogramming and small RNA silencing of transposable elements in pollen. *Cell* **136**, 461-472.
Sniezko, R. (2006) Meiosis in plants. In *Plant Cell Biology* (ed. W. V. Dashek and P. Harrison). Enfield, NH: Science Publisher.
Talbert, P. B., Masuelli, R., Tyagi, A. P., Comai, L. and Henikoff, S. (2002). Centromeric localization and adaptive evolution of an Arabidopsis histone H3 variant. *Plant Cell* **14**, 1053-1066.
Terme, J. M., Sesé, B., Millán-Ariño, L., Mayor, R., Izpisúa Belmonte, J. C., Barrero, M. J. and Jordan, A. (2011). Histone H1 variants are differentially expressed and incorporated into chromatin during differentiation and reprogramming to pluripotency. *J. Biol. Chem.* **286**, 35347-35357.
Tessadori, F., Chupeau, M. C., Chupeau, Y., Knip, M., Germann, S., van Driel, R., Fransz, P. and Gaudin, V. (2007). Large-scale dissociation and sequential reassembly of pericentric heterochromatin in dedifferentiated Arabidopsis cells. *J. Cell Sci.* **120**, 1200-1208.
Thorstensen, T., Grini, P. E. and Aalen, R. B. (2011). SET domain proteins in plant development. *Biochim. Biophys. Acta* **1809**, 407-420.
Tian, L., Fong, M. P., Wang, J. J., Wei, N. E., Jiang, H., Doerge, R. W. and Chen, Z. J. (2005). Reversible histone acetylation and deacetylation mediate genome-wide, promoter-dependent and locus-specific changes in gene expression during plant development. *Genetics* **169**, 337-345.
Tiang, C. L., He, Y. and Pawlowski, W. P. (2012). Chromosome organization and dynamics during interphase, mitosis, and meiosis in plants. *Plant Physiol.* **158**, 26-34.
Tucker, M. R., Okada, T., Hu, Y., Scholefield, A., Taylor, J. M. and Koltunow, A. M. (2012). Somatic small RNA pathways promote the mitotic events of megagametogenesis during female reproductive development in Arabidopsis. *Development* **139**, 1399-1404.
Turck, F., Roudier, F., Farrona, S., Martin-Magniette, M. L., Guillaume, E., Buisine, N., Gagnot, S., Martienssen, R. A., Coupland, G. and Colot, V. (2007). Arabidopsis TFL2/LHP1 specifically associates with genes marked by trimethylation of histone H3 lysine 27. *PLoS Genet.* **3**, e86.
Vaillant, I. and Paszkowski, J. (2007). Role of histone and DNA methylation in gene regulation. *Curr. Opin. Plant Biol.* **10**, 528-533.
Vaquero-Sedas, M. I., Gámez-Arjona, F. M. and Vega-Palas, M. A. (2011). Arabidopsis thaliana telomeres exhibit euchromatic features. *Nucleic Acids Res.* **39**, 2007-2017.
Veiseth, S. V., Rahman, M. A., Yap, K. L., Fischer, A., Egge-Jacobsen, W., Reuter, G., Zhou, M. M., Aalen, R. B. and Thorstensen, T. (2011). The SUVR4 histone lysine methyltransferase binds ubiquitin and converts H3K9me1 to H3K9me3 on transposon chromatin in Arabidopsis. *PLoS Genet.* **7**, e1001325.
Wierzbicki, A. T. and Jerzmanowski, A. (2005). Suppression of histone H1 genes in Arabidopsis results in heritable developmental defects and stochastic changes in DNA methylation. *Genetics* **169**, 997-1008.
Williams, L., Zhao, J., Morozova, N., Li, Y., Avivi, Y. and Grafi, G. (2003). Chromatin reorganization accompanying cellular dedifferentiation is associated with modifications of histone H3, redistribution of HP1, and activation of E2F-target genes. *Dev. Dyn.* **228**, 113-120.
Wollmann, H., Holec, S., Alden, K., Clarke, N. D., Jacques, P. E. and Berger, F. (2012). Dynamic deposition of histone variant H3.3 accompanies developmental remodeling of the Arabidopsis transcriptome. *PLoS Genet.* **8**, e1002658.
Wuest, S. E., Schmid, M. W. and Grossniklaus, U. (2013). Cell-specific expression profiling of rare cell types as exemplified by its impact on our understanding of female gametophyte development. *Curr. Opin. Plant Biol.* **16**, 41-49.
Yang, W. C. and Sundaresan, V. (2000). Genetics of gametophyte biogenesis in Arabidopsis. *Curr. Opin. Plant Biol.* **3**, 53-57.
Yang, S. M., Kim, B. J., Norwood Toro, L. and Skoultchi, A. I. (2013). H1 linker histone promotes epigenetic silencing by regulating both DNA methylation and histone H3 methylation. *Proc. Natl. Acad. Sci. USA* **110**, 1708-1713.
Yelina, N. E., Choi, K., Chelysheva, L., Macaulay, M., de Snoo, B., Wijnker, E., Miller, N., Drouaud, J., Grelon, M., Copenhaver, G. P. et al. (2012). Epigenetic remodeling of meiotic crossover frequency in Arabidopsis thaliana DNA methyltransferase mutants. *PLoS Genet.* **8**, e1002844.
Zemach, A., Kim, M. Y., Hsieh, P. H., Coleman-Derr, D., Eshed-Williams, L., Thao, K., Harmer, S. L. and Zilberman, D. (2013). The Arabidopsis nucleosome remodeler DDM1 allows DNA methyltransferases to access H1-containing heterochromatin. *Cell* **153**, 193-205.
Zhang, W., Lee, H. R., Koo, D. H. and Jiang, J. (2008). Epigenetic modification of centromeric chromatin: hypomethylation of DNA sequences in the CENH3-associated chromatin in Arabidopsis thaliana and maize. *Plant Cell* **20**, 25-34.
Zhao, J., Morozova, N., Williams, L., Libs, L., Avivi, Y. and Grafi, G. (2001). Two phases of chromatin decondensation during dedifferentiation of plant cells: distinction between competence for cell fate switch and a commitment for S phase. *J. Biol. Chem.* **276**, 22772-22778.
Zhu, Y., Dong, A., Meyer, D., Pichon, O., Renou, J. P., Cao, K. and Shen, W. H. (2006). Arabidopsis NRP1 and NRP2 encode histone chaperones and are required for maintaining postembryonic root growth. *Plant Cell* **18**, 2879-2892.
Zilberman, D. (2008). The evolving functions of DNA methylation. *Curr. Opin. Plant Biol.* **11**, 554-559.